Mapping permeability over the surface of the Earth

Tom Gleeson,[1] Leslie Smith,[1] Nils Moosdorf,[2] Jens Hartmann,[2] Hans H. Dürr,[3] Andrew H. Manning,[4] Ludovicus P. H. van Beek,[3] and A. M. Jellinek[1]

Received 20 September 2010; revised 10 November 2010; accepted 23 November 2010; published 21 January 2011.

[1] Permeability, the ease of fluid flow through porous rocks and soils, is a fundamental but often poorly quantified component in the analysis of regional-scale water fluxes. Permeability is difficult to quantify because it varies over more than 13 orders of magnitude and is heterogeneous and dependent on flow direction. Indeed, at the regional scale, maps of permeability only exist for soil to depths of 1–2 m. Here we use an extensive compilation of results from hydrogeologic models to show that regional-scale (>5 km) permeability of consolidated and unconsolidated geologic units below soil horizons (hydrolithologies) can be characterized in a statistically meaningful way. The representative permeabilities of these hydrolithologies are used to map the distribution of near-surface (on the order of 100 m depth) permeability globally and over North America. The distribution of each hydrolithology is generally scale independent. The near-surface mean permeability is of the order of $\sim 5 \times 10^{-14}$ m^2. The results provide the first global picture of near-surface permeability and will be of particular value for evaluating global water resources and modeling the influence of climate-surface-subsurface interactions on global climate change. **Citation:** Gleeson, T., L. Smith, N. Moosdorf, J. Hartmann, H. H. Dürr, A. H. Manning, L. P. H. van Beek, and A. M. Jellinek (2011), Mapping permeability over the surface of the Earth, *Geophys. Res. Lett.*, *38*, L02401, doi:10.1029/2010GL045565.

1. Introduction

[2] Estimating and mapping regional-scale permeability is critical to examining diverse earth processes and addressing water resource problems. Land-surface, subsurface and climate models have been used to examine interactions between groundwater, soil moisture, surface water and climate [*York et al.*, 2002; *Liang and Xie*, 2003; *Yeh and Eltahir*, 2005; *Fan et al.*, 2007; *Miguez-Macho et al.*, 2007; *Anyah et al.*, 2008; *Maxwell and Kollet*, 2008] and the response of aquifers to climate change [*Scibek and Allen*, 2006]. However the integration of groundwater systems into large-scale earth system models has been limited by the lack of available parameter data, most acutely permeability data. Soil permeability (~1–2 m depth) has been mapped over North America [*Fan et al.*, 2007] but the permeability of lithologies underlying soil has not been systematically examined or mapped. Mapping regional-scale permeability also addresses groundwater resource concerns because permeability, along with recharge rate and hydraulic gradient, governs the flux through aquifers. Finally, permeability affects a myriad of deeper earth process [*Ingebritsen et al.*, 2006] including volcanism and earthquakes [*Wang and Manga*, 2010], the formation of metallic mineral deposits and oil resources [*Garven*, 1995; *Person et al.*, 1996], crustal-scale metamorphic fluid flow [*Lyubetskaya and Ague*, 2009] and the development of abnormal fluid pressures in basins [*Neuzil*, 1994]. Here we compile for the first time regional-scale permeability values for diverse lithologies in order to estimate and map near-surface permeability.

2. Methods

2.1. Permeability Compilation

[3] Our focus is the permeability of saturated terrestrial lithologies rather than unsaturated permeability which is non-linear and transient, or the permeability of oceanic lithologies which were previously compiled [*Fisher*, 1998]. We define local- and regional-scale permeability based on the scale and method of quantification. At a local scale (<1 m to 1 km) permeability is quantified using hydraulic tests [*Freeze and Cherry*, 1979; *Hsieh*, 1998]. The estimates of permeability for individual lithologies (Figure 1a) are generally consistent between local-scale compilations [*Davis*, 1969; *Freeze and Cherry*, 1979; *Brace*, 1980] and we do not further compile or examine local-scale permeability data. Regional-scale permeability has only been previously compiled for crystalline and fine-grained siliciclastic sedimentary rock [*Clauser*, 1992; *Neuzil*, 1994; *Hsieh*, 1998]. Permeability at a regional scale can only be quantified through calibration of numerical models to hydraulic, streamflow, chemical or thermal observations. We define regional scale as >5 km to ensure that we are well above the scale at which heterogeneities such as discrete fractures control groundwater flow. We also define hydrolithologies as broad lithologic categories with similar hydrogeologic characteristics such as permeability. Geologic units (from geologic maps or hydrogeological models) are categorized into hydrolithologies. Our hydrolithologic categorization is consistent with current hydrogeologic modeling practice and is an extension of the 'hydrostratigraphic' concept commonly employed in hydrogeologic modeling of sedimentary basins [*Person et al.*, 1996].

[4] We compiled two-hundred and thirty hydrogeologic units from calibrated models which are grouped into seven hydrolithologic categories (Table S1 and Methods in the auxiliary material).[1] Also, two combined hydrolithologic

[1]Department of Earth and Ocean Sciences, University of British Columbia, Vancouver, British Columbia, Canada.
[2]Institute for Biogeochemistry and Marine Chemistry, Klim Campus, University of Hamburg, Hamburg, Germany.
[3]Department of Physical Geography, Faculty of Geosciences, Utrecht University, Utrecht, Netherlands.
[4]U.S. Geological Survey, Denver, Colorado, USA.

0094-8276/11/2010GL045565

[1]Auxiliary materials are available in the HTML. doi:10.1029/2010GL045565.

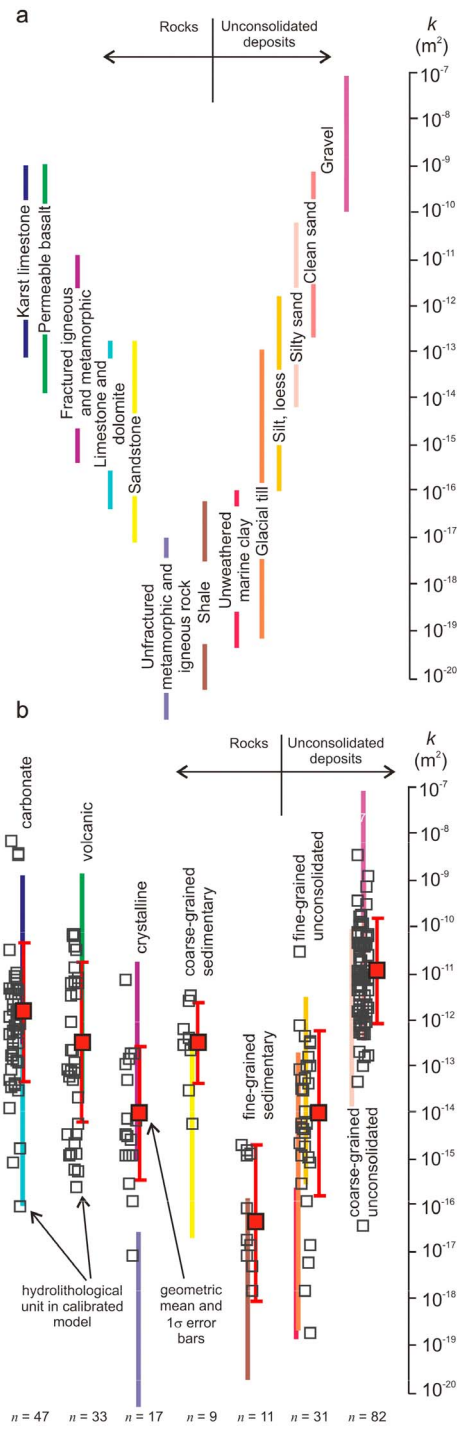

Figure 1. Comparing (a) local-scale permeability (k) ranges from *Freeze and Cherry* [1979] and (b) calibrated regional-scale hydrogeologic models. Each open square represents a hydrolithologic unit in a calibrated model that is larger than 5 km horizontally. In Figure 1b local-scale permeability ranges are shown behind the open squares by the same colored bars. Values are grouped into hydrolithologic categories (i.e., fine grained unconsolidated). The geometric mean for each hydrolithologic category is shown as a red square with the red line representing the 1σ standard deviation for each hydrolithologic category.

categories (i.e., unconsolidated and siliciclastic sedimentary), used later in mapping, are defined in Table 1 as amalgamations of four hydrolithologic categories. Only hydrogeologic units that occur at shallow depths (<100 m) are included because permeabilities are later integrated with lithologies mapped from surface exposures and permeability is depth-dependent [*Ingebritsen and Manning*, 1999; *Saar and Manga*, 2004; *Ingebritsen and Manning*, 2010; *Jiang et al.*, 2010]. The normality of the raw, logarithmic permeability (log k) values (categorized by hydrolithology) was tested by the Kolmogorov-Smirnov (K-S distribution) and Shapiro-Wilk (W-statistic) tests. For a particular location or site, effective (larger-scale) permeability is often considered to be best represented by the geometric mean of local-scale measurements [*Zinn and Harvey*, 2003]. There is currently no established framework for estimating effective permeability of data from different locations as we have compiled in Table S1. We adopt the geometric mean of permeability values as the best estimate of regional-scale permeability for the hydrolithologies and combined hydrolithologies (Table 1).

2.2. Permeability Mapping

[5] Near-surface permeability maps over the globe and North America are derived by attributing lithology maps with the geometric mean permeability of each lithology (see Methods in the auxiliary material). Global and North American lithology maps are derived directly from bedrock and unconsolidated (surficial) geology maps by classifying geologic units into lithologic categories [*Dürr et al.*, 2005; *Jansen et al.*, 2010; *Moosdorf et al.*, 2010] (Table 1). The global map has 15 lithology categories and is spatially continuous at a coarse resolution (12,857 km^2 mean polygon area for 1472 polygons in North America)[*Dürr et al.*, 2005]. The 15 lithologic categories are paired with five 'combined hydrolithologies' (Table 1). The lithology of North America is mapped in much greater detail (75 km^2 mean polygon area for 262,111 polygons) than the global map and lithologies are divided into eight sub-lithologies but the map is derived from a variety of digital sources resulting in artifacts at some administrative boundaries [*Jansen et al.*, 2010; *Moosdorf et al.*, 2010]. The sub-lithologies are paired with the hydrolithologies that divide unconsolidated and siliciclastic sedimentary categories (Table 1). The permeability maps assume that 1) each hydrolithology has a representative, scale-independent, regional-scale permeability; 2) hydrolithologies can be paired with lithologies; and 3) lithology maps represent the geology of the shallow subsurface accurately and consistently.

[6] Previous maps of permeability [*Luo et al.*, 2010] are too detailed for comparison so we test the reliability of the permeability maps using aquifer maps since aquifers coincide with units of higher permeability material. The U.S. Geological Survey has mapped aquifers in detail [*U.S. Geological Survey*, 2003] (1536 km^2 mean polygon area for 3010 polygons in the conterminous United States). The resolution of global aquifer mapping is too coarse to analyze (75,078 km^2 mean polygon area for 369 polygons in North America) [*BGR and UNESCO*, 2008]. Finally, we derive the spatially-distributed mean permeability for North America and the globe from a raster calculation that compensates for the spatial distribution (size and frequency)

Table 1. Hydrolithologic and Lithologic Categories[a]

	log$k$ μ_{geo} (m^2)	log$k$ σ (m^2)	n	W	p	K-S	p	Lithology[b]	Sub-lithology[c]
Combined Hydrolithology (Global Map)									
unconsolidated	−13.0	2.0	113	**0.919**	**<0.001**	**0.122**	**<0.001**	AD, DS, LO, SU	
sil. sedimentary	−15.2	2.5	20	0.942	0.265	0.154	>0.2	SS, SM, CL	
carbonate	−11.8	1.5	47	**0.931**	**0.0008**	**0.142**	**0.019**	SC	
crystalline	−14.1	1.5	17	0.972	0.852	0.135	>0.2	MT, PA, PB, PR	
volcanic	−12.5	1.8	33	**0.933**	**0.043**	0.134	0.136	VA,VB	
not assigned	-	-		-	-	-	-	WB, IG, EV	
Hydrolithology (North America Map)									
c.g. unconsolidated	−10.9	1.2	82	**0.93**	**<0.001**	0.078	>0.2	AD, DS, LO, SU	SS
f.g. unconsolidated	−14.0	1.8	31	0.955	0.209	0.121	>0.2	AD, DS, LO, SU	SH
unconsolidated	−13.0	2.0	113	**0.919**	**<0.001**	**0.122**	**<0.001**	AD, DS, LO, SU	MX, PY
c.g. sil. sedimentary	−12.5	0.9	9	0.923	0.417	0.234	0.164	SS, SM	SS
f.g. sil. sedimentary	−16.5	1.7	11	0.89	0.141	0.186	>0.2	SS, SM	SH
sil. sedimentary	−15.2	2.5	20	0.942	0.265	0.154	>0.2	SS, SM	MX, PY, AM, GR
carbonate	−11.8	1.5	47	**0.931**	**0.0008**	**0.142**	**0.019**	SC	
crystalline	−14.1	1.5	17	0.972	0.852	0.135	>0.2	MT, PA, PB	PI
volcanic	−12.5	1.8	33	**0.933**	**0.043**	0.134	0.136	VA,VB	VI, PY
not assigned	-	-		-	-	-	-	WB, IG, EV	

[a]log$k$ μ_{geo} is the geometric mean logarithmic permeability; σ is the standard deviation; n is the number of hydrolithologic units; W is the Shapiro-Wilk statistic; p is the p-value for $\alpha = 0.05$; K-S is the Kolmogorov-Smirnov distribution; sil. sedimentary is siliciclastic sedimentary; c.g. and f.g. are coarse- and fine-grained, respectively; values in bold fail normality test ($p < \alpha$).

[b]*Dürr et al.* [2005] divided lithologies globally into alluvial (AD), dune sands (DS), evaporites (EV), loess (LO), unconsolidated sediments (SU), carbonate sedimentary rocks (SC), mixed sedimentary rocks (SM), siliciclastic sedimentary rocks (SS), metamorphic rocks (MT), acid plutonic rocks (PA), basic plutonic rocks (PB), acid volcanic rocks (VA), basic volcanic rocks (VB), Precambrian basement (PR), complex lithologies (CL), water bodies (WB) and ice and glaciers (IG).

[c]*Jansen et al*. [2010] mapped North America using the same lithologic categories (except for PR and CL) as *Dürr et al.* [2005] and the following subcategories described by *Moosdorf et al*. [2010]: sandstone or coarse dominates clastic fraction (SS), shale or siltstone dominates clastic fraction (SH), no grain size domination distinguishable (MX), pyroclastics mentioned (PY), amphibolite mentioned (AM), greenstone mentioned (GR), intermediate plutonic rocks (PI) and intermediate volcanic rocks (VI).

of each hydrolithologic unit (see Methods in the auxiliary material).

3. Results and Discussion

[7] Figure 1 indicates that regional-scale permeabilities from calibrated models are consistent with local-scale ranges. Figure 1b illustrates our compilation of calibrated, regional-scale hydrogeological models from a variety of hydrogeological settings and calibration targets. The logarithmic permeability (log k) results categorized by hydrolithology (Table S1) are generally normally distributed at the 95% confidence level ($\alpha = 0.05$) as indicated by two normality tests, although we recognize the limitations of these tests including the limited data of some hydrolithologies. Seven of nine and five of nine hydrolithologic and combined hydrolithologic categories passed the Kolmogorov-Smirnov (K-S distribution) and Shapiro-Wilk (W-statistic) normality tests, respectively (Table 1). The categories that failed have outliers (Figure 1), which may be a result of integrating a variety of hydrogeologic characteristics, such as karst and non-karst carbonates, into a single category. Dividing the hydrolithologic categories into subcategories is not possible due to data availability. For example, the degree of karst development is not systematically documented in hydrogeologic models. The standard deviation of hydrolithologies and combined hydrolithologies are 1–2 and 2–2.5 orders of magnitude, respectively (Table 1). At both local scale and regional scale, order of magnitude accuracy of permeability can be useful since permeability ranges over greater than 13 orders of magnitude [*Freeze and Cherry*, 1979]. Therefore our estimates of regional-scale permeability are useful although the spread in the data is complex for some hydrolithologies (Figures 1 and 2). To maintain a consistent metric across all hydrolithologies we adopt the geometric mean as the best estimate of regional-scale permeability.

[8] An important question for mapping is whether permeability is independent of scale for each hydrolithology. Previous compilations and observations suggest that regional-scale permeability may not be scale dependent for crystalline rocks [*Clauser*, 1992; *Hsieh*, 1998; *Ingebritsen et al.*, 2006]. Similarly, there is no discernable dependence of permeability on scale (i.e. length of the hydrolithologic unit) for crystalline rocks in our compilation (Figure 2a) or for other hydrolithologies (Figure 2b shows coarse-grained unconsolidated hydrolithology as an example). The only hydrolithogy that is an exception is carbonates (Figure 2c) where permeability increases with scale, possibly due to karst [*Halihan et al.*, 2000] or sampling bias. Therefore, the geometric mean can represent large areas (5–100 km in length) and are not scale dependent in this range for all hydrolithologies except carbonates. Since carbonates represent a small surface area (10% globally or for North America) [*Dürr et al.*, 2005; *Jansen et al.*, 2010] we assume that all hydrolithologies are scale-independent for the mapping described below.

[9] Figure 3 shows regional-scale permeability over the globe and North America derived by attributing lithology maps with the geometric mean permeability of each hydrolithology. The differences in lithologic mapping and hydrolithologic categorization result in differences in the permeability maps. The global map (Figure 3a) is continuous but coarsely resolved whereas the permeability map for North America is more refined and higher-resolution but has minor artifacts

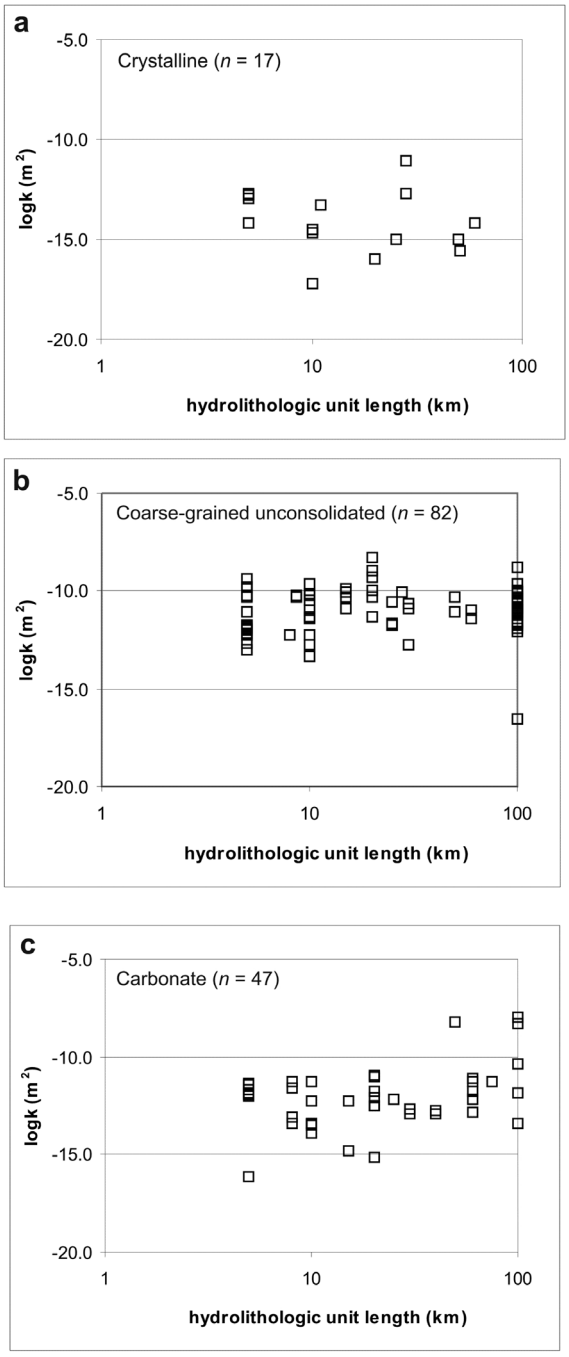

Figure 2. The relationship between permeability and scale of hydrolithologic units for (a) crystalline rocks, (b) coarse-grained unconsolidated sediments and (c) carbonate rocks. The horizontal unit length is recorded as 100 km if greater than 100 km.

at some administrative boundaries (Figure 3c). Over North America, both permeability maps have a similar distribution of permeability but the more detailed map of North America has a greater range of permeability values since different grain size are distinguished within the unconsolidated and siliciclastic sedimentary categories. The North America permeability map is consistent with the U.S. Geological Survey aquifer map since the areas mapped as aquifers generally have a higher permeability (Figure S1). Both permeability maps have inherent uncertainty represented by the standard deviation of the individual hydrolithologies. The standard deviation of the global map (Figure 3b) is generally larger than the North American map (Figure 3d) since different grain sizes of unconsolidated and siliciclastic sedimentary categories are not distinguished on the global map (Table 1).The spatially-distributed mean logarithmic permeabilities (log$k$) for the globe and North America are -13.2 ± 2.7 m^2 and -13.5 ± 3.1 m^2, respectively, which is consistent with previous estimates of shallow crustal permeability [*Brace*, 1980; *Ingebritsen and Manning*, 1999].

[10] Depending on the application of the permeability maps various caveats may be important, in addition to the assumptions listed in Section 2.2. First, we focus on saturated permeability but saturation varies over the earth surface. Unsaturated permeabilities can be much lower than saturated permeabilities and are transient and non-linear depending on lithology and water saturation. To use these permeability maps in earth system models of regions where unsaturated zone processes are predominant, the relative permeability or constitutive relations between pressure and saturation [e.g., *Brooks and Corey*, 1964; *van Genuchten*, 1980] must also be defined. Second, the depths that the permeability maps represent are connected to the depths for which the surface lithologic condition represents the subsurface. We estimate that the lithology maps represent the shallow subsurface (on the order of 100 m) although specific depth estimates could be misleading in some areas due to variations in unit thickness, diagenesis or weathering. Third, defining spatially-distributed permeability at greater depths remains a significant challenge that is crucial to examining deeper earth processes and the coupling between shallow and deep earth processes. One possibility could involve using the permeability estimates in Figure 1 and Table 1 with simple permeability-depth relations [*Ingebritsen and Manning*, 1999; *Ingebritsen and Manning*, 2010; *Jiang et al.*, 2010] to examine and model deeper earth processes. Fourth, permeability north of the continuous permafrost line (Figure 3) [*Brown et al.*, 2001] will be considerably lower than the mapped permeability which assumes ice-free conditions. Fifth, the near-surface permeability may not be well represented in tropical regions where bedrock has been mapped and significantly weathered *in situ*. Finally, the North America map has artifacts at some administrative boundaries whereas the global map is continuous.

4. Conclusions

[11] By combining recent lithology maps with a compilation of near-surface permeability values it is possible to: 1) resolve the heterogeneity of permeability into permeability values that represent specific geological materials (Figure 1b) and 2) map permeability at new scales and to greater depths than an approach based on soil classification (Figure 3). The permeability maps and estimates will likely be most useful for large-scale earth system models and/or for estimation of permeability in regions with sparse permeability data. Quantifying spatially-distributed permeability will improve representation of the groundwater component of the hydrologic cycle in earth system models as well as evaluation of direct and indirect human modifications to the hydrologic cycle.

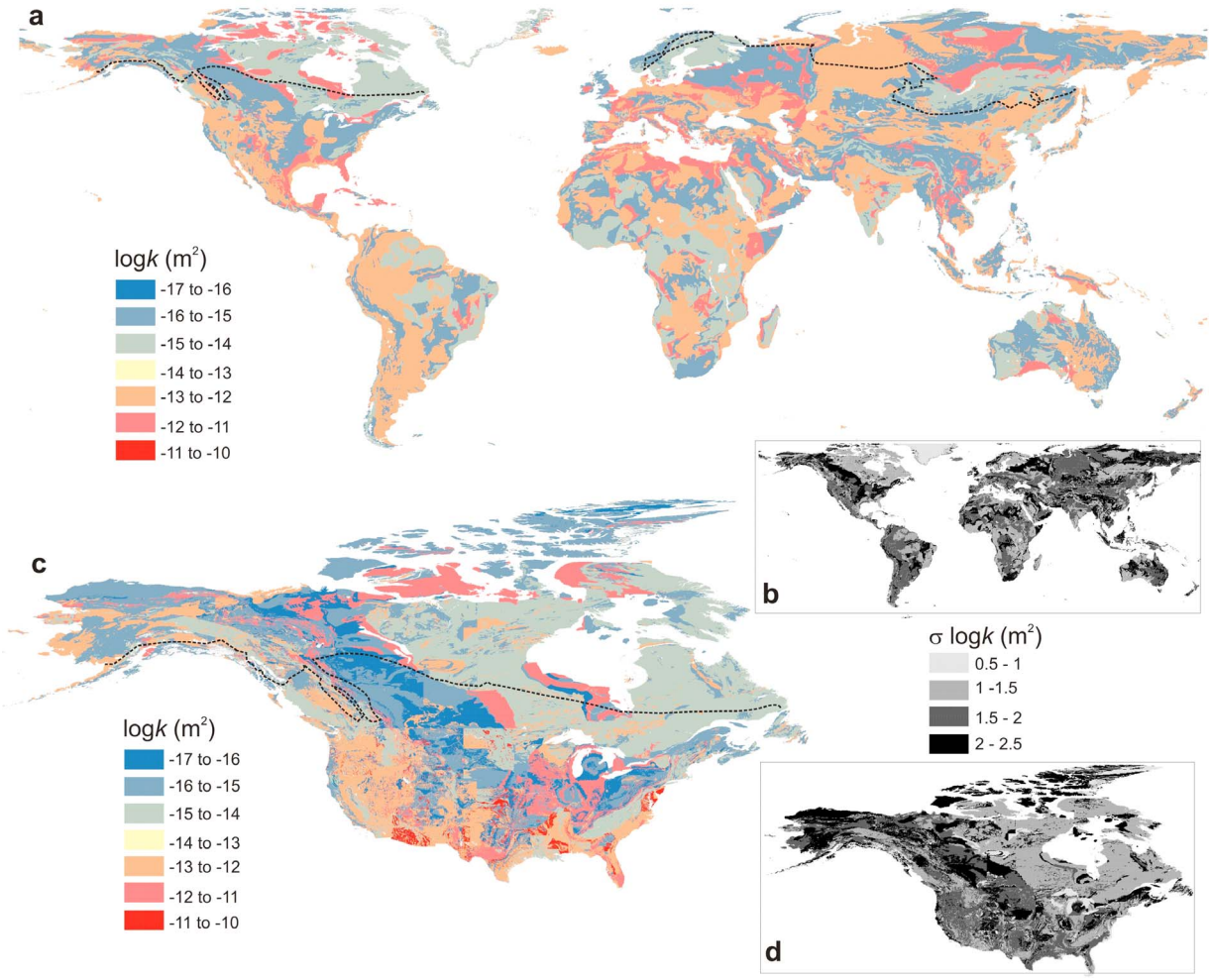

Figure 3. Mapping logarithmic permeability (log$k$ m^2) and uncertainty over the globe and North America. Global distribution of (a) permeability and (b) uncertainty. Distribution of (c) permeability and (d) uncertainty over North America (excluding Mexico). Regional-scale permeability will be much lower in the regions north of the dashed continuous permafrost line [*Brown et al.*, 2001]. Smaller continuous permafrost areas in mountainous terrain are not shown. See Figure S2 for larger versions of Figures 3b and 3d.

[12] **Acknowledgments.** TG is supported by a NSERC postdoctoral grant. JH and NM are supported through the German Science Foundation (DFG-project HA 4472/6-1 and the Cluster of Excellence 'CliSAP' (EXC177), University of Hamburg). We thank numerous hydrogeologists including L.Bentley, B.Jaworska-Szulc, C.Neuzil, A. Reeves, R.Rojas-Mujica and W.Sanford for providing information for the compilation. N. Sihota completed the normality tests. J.Caine (USGS), K.Christie (University of Alaska-Fairbanks), H.Peterson (UBC) and D.Sweetkind (USGS) and two anonymous reviewers greatly improved this paper. Please contact TG to contribute to the ongoing permeability compilation or for high-resolution versions of the permeability map. HHD has been funded by Utrecht University (High Potential Project G-NUX) and the EU FP6 project CARBO-North (project number 036993).

References

Anyah, R. O., C. P. Weaver, G. Miguez-Macho, Y. Fan, and A. Robock (2008), Incorporating water table dynamics in climate modeling: 3. Simulated groundwater influence on coupled land-atmosphere variability, *J. Geophys. Res.*, *113*, D07103, doi:10.1029/2007JD009087.

BGR and UNESCO (2008), Groundwater resources of the world, scale 1:25 000 000, WHYMAP, Hanover, Germany.

Brace, W. F. (1980), Permeability of crystalline and argillaceous rocks, *Int. J. Mech. Min. Sci. Geomech. Abstr.*, *17*, 241–251, doi:10.1016/0148-9062(80)90807-4.

Brooks, R. H., and A. T. Corey (1964), Hydraulic properties of porous media, *Hydrol. Pap. 3*, Univ. of Colo., Fort Collins.

Brown, J., et al. (2001), Circum-arctic map of permafrost and ice ground conditions, Natl. Snow and Ice Data Cent., Boulder, Colo.

Clauser, C. (1992), Permeability of crystalline rocks, *Eos Trans. AGU*, *73*(21), 233, doi:10.1029/91EO00190.

Davis, S. N. (1969), Porosity and permeability of natural materials, in *Flow Through Porous Media*, edited by R. J. M. De Wiest, pp. 53–90, Academic, New York.

Dürr, H. H., M. Meybeck, and S. H. Dürr (2005), Lithologic composition of the Earth's continental surfaces derived from a new digital map emphasizing riverine material transfer, *Global Biogeochem. Cycles*, *19*, GB4S10, doi:10.1029/2005GB002515.

Fan, Y., G. Miguez-Macho, C. P. Weaver, R. Walko, and A. Robock (2007), Incorporating water table dynamics in climate modeling: 1. Water table observations and equilibrium water table simulations, *J. Geophys. Res.*, *112*, D10125, doi:10.1029/2006JD008111.

Fisher, A. T. (1998), Permeability within basaltic oceanic crust, *Rev. Geophys.*, *36*(2), 143–182, doi:10.1029/97RG02916.

Freeze, R. A., and J. A. Cherry (1979), *Groundwater*, 604 pp., Prentice-Hall, Englewood Cliffs, N. J.

Garven, G. (1995), Continental-scale groundwater flow and geologic processes, *Annu. Rev. Earth Planet. Sci.*, *23*, 89–117, doi:10.1146/annurev.ea.23.050195.000513.

Halihan, T., et al. (2000), Flow in the San Antonio segment of the Edwards aquifer: matrix, fractures, or conduits?, in *Groundwater Flow and Contaminant Transport in Carbonate Aquifers*, edited by I. D. Sasowsky and C. M. Wicks, pp. 129–145, Balkema, Rotterdam, Netherlands.

Hsieh, P. A. (1998), Scale effects in fluid flow through fractured geologic media, in *Scale Dependence and Scale Independence in Hydrology*, edited by G. Sposito, pp. 335–353, Cambridge Univ. Press, Cambridge, U. K., doi:10.1017/CBO9780511551864.013.

Ingebritsen, S. E., and C. E. Manning (1999), Geological implications of a permeability-depth curve for the continental crust, *Geology*, *27*, 1107–1110, doi:10.1130/0091-7613(1999)027<1107:GIOAPD>2.3.CO;2.

Ingebritsen, S. E., and C. E. Manning (2010), Permeability of the continental crust: Dynamic variations inferred from seismicity and metamorphism, *Geofluids*, *10*, 193–205.

Ingebritsen, S. E., et al. (2006), *Groundwater in Geological Processes*, 562 pp., Cambridge Univ. Press, Cambridge, U. K.

Jansen, N., et al. (2010), Dissolved silica mobilization in the conterminous USA, *Chem. Geol.*, *270*, 90–109, doi:10.1016/j.chemgeo.2009.11.008.

Jiang, X.-W., et al. (2010), Semi-empirical equations for the systematic decrease in permeability with depth in porous and fractured media, *Hydrogeol. J.*, *18*, 839–850, doi:10.1007/s10040-010-0575-3.

Liang, X., and Z. Xie (2003), Important factors in land-atmosphere interactions: Surface runoff generations and interactions between surface and groundwater, *Global Planet. Change*, *38*, 101–114, doi:10.1016/S0921-8181(03)00012-2.

Luo, W., et al. (2010), Estimating hydraulic conductivity from drainage patterns—A case study in the Oregon Cascades, *Geology*, *38*, 335–338, doi:10.1130/G30816.1.

Lyubetskaya, T., and J. J. Ague (2009), Modeling the magnitudes and directions of regional metamorphic fluid flow in collisional orogens, *J. Petrol.*, *50*, 1505–1531, doi:10.1093/petrology/egp039.

Maxwell, R. M., and S. J. Kollet (2008), Interdependence of groundwater dynamics and land-energy feedbacks under climate change, *Nat. Geosci.*, *1*, 665–669, doi:10.1038/ngeo315.

Miguez-Macho, G., Y. Fan, C. P. Weaver, R. Walko, and A. Robock (2007), Incorporating water table dynamics in climate modeling: 2. Formulation, validation, and soil moisture simulation, *J. Geophys. Res.*, *112*, D13108, doi:10.1029/2006JD008112.

Moosdorf, N., J. Hartmann, and H. H. Dürr (2010), Lithological composition of the North American continent and implications of lithological map resolution for dissolved silica flux modeling, *Geochem. Geophys. Geosyst.*, *11*, Q11003, doi:10.1029/2010GC003259.

Neuzil, C. E. (1994), How permeable are clays and shales?, *Water Resour. Res.*, *30*, 145–150, doi:10.1029/93WR02930.

Person, M., J. P. Raffensperger, S. Ge, and G. Garven (1996), Basin-scale hydrogeologic modeling, *Rev. Geophys.*, *34*, 61–87, doi:10.1029/95RG03286.

Saar, M. O., and M. Manga (2004), Depth dependence of permeability in the Oregon Cascades inferred from hydrogeologic, thermal, seismic, and magmatic modeling constraints, *J. Geophys. Res.*, *109*, B04204, doi:10.1029/2003JB002855.

Scibek, J., and D. M. Allen (2006), Modeled impacts of predicted climate change on recharge and groundwater levels, *Water Resour. Res.*, *42*, W11405, doi:10.1029/2005WR004742.

U.S. Geological Survey (2003), Principal aquifers of the 48 conterminous United States, Hawaii, Puerto Rico, and the U.S. Virgin Islands, U.S. Geol. Surv., Reston, Va.

van Genuchten, M. T. (1980), A closed-form equation for predicting the hydraulic conductivity of unsaturated soils, *Soil Sci. Soc. Am. J.*, *24*, 133–144.

Wang, C.-Y., and M. Manga (2010), *Earthquakes and Water*, 218 pp., Springer, Berlin.

Yeh, P. J. F., and E. A. B. Eltahir (2005), Representation of water table dynamics in a land surface scheme. Part I: Model development, *J. Clim.*, *18*, 1861–1880, doi:10.1175/JCLI3330.1.

York, J. P., et al. (2002), Putting aquifers into atmospheric simulation models: An example from the Mill Creek Watershed, northeastern Kansas, *Adv. Water Resour.*, *25*, 221–238, doi:10.1016/S0309-1708(01)00021-5.

Zinn, B., and C. F. Harvey (2003), When good statistical models of aquifer heterogeneity go bad: A comparison of flow, dispersion, and mass transfer in connected and multivariate Gaussian hydraulic conductivity fields, *Water Resour. Res.*, *39*(3), 1051, doi:10.1029/2001WR001146.

H. H. Dürr and L. P. H. van Beek, Department of Physical Geography, Faculty of Geosciences, Utrecht University, PO Box 80115, NL-3508 TC Utrecht, Netherlands.

T. Gleeson, A. M. Jellinek, and L. Smith, Department of Earth and Ocean Sciences, University of British Columbia, 6339 Stores Rd., Vancouver, BC V6T 1Z4, Canada. (tgleeson@eos.ubc.ca)

J. Hartmann and N. Moosdorf, Institute for Biogeochemistry and Marine Chemistry, Klim Campus, University of Hamburg, Bundesstraße 55, D-20146 Hamburg, Germany.

A. H. Manning, U.S. Geological Survey, PO Box 25046, Mail Stop 973, Denver, CO 80225-0046, USA.